ACS Sustainable Chemistry & Engineering

Research Article

pubs.acs.org/journal/ascecg

Multiparameters Model of the Initial SOC Considering the Relaxation Effect

Yanhui Zhang,[†,‡] Wenji Song,*[,†] Shili Lin,[†] and Ziping Feng[†]

[†]Key Laboratory of Renewable Energy, Guangzhou Institute of Energy Conversion, Chinese Academy of Sciences, Guangzhou 510640, P. R. China

[‡]University of Chinese Academy of Sciences, Beijing 10049, P. R. China

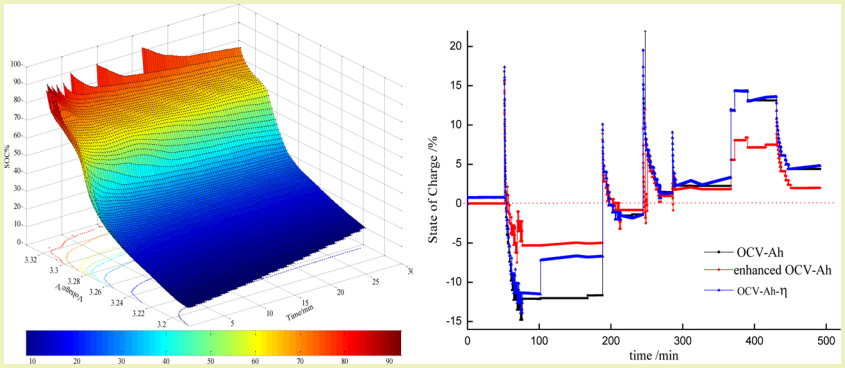

ABSTRACT: To improve the accuracy of the initial state-of-charge (SOC_0) estimation, an enhanced SOC_0 model-based ampere-hour (Ah) model of a $LiFePO_4$ battery is presented for application in a battery energy storage system. It varies as a function of the open circuit voltage (OCV), rates, and relaxation effect. Here, the Thevenin equivalent circuit model is selected to model the $LiFePO_4$ battery, and its mathematic equations are deduced to determine the inherent trade-off between the time constant and main parameter of the battery, which can address the dilemma of the conventional SOC_0 method (OCV model) as the relaxation effect and how long the battery takes to reach a steady state. To illustrate advantages of the enhanced estimation model, a comparison analysis is performed on the enhanced model with the former model under the dynamic stress test. Furthermore, the experimental results indicate that the correction of SOC_0 can significantly decrease the estimation error. The enhanced SOC_0 model is expected to help determine operational parameters for batteries of variable power sources.

KEYWORDS: *Battery, Battery models, Initial state-of-charge (SOC_0), State-of-charge (SOC)*

INTRODUCTION

The lithium-ion battery has attracted special attention for consumer electronics owing to its advantages of high specific power, high energy density, no memory effect, and long durability.[1] Besides consumer electronics, it is also growing in popularity for aerospace, hybrid electric vehicle (HEV), electric vehicle (EV), and military applications. Meanwhile, research is yielding a series of improvements to traditional battery manufacturing technology, focusing on energy density and intrinsic safety.

A battery management system (BMS), along with the monitoring unit and communication bus, is an important means for raising the intrinsic safety and durability of batteries. One of the greatest challenges among the main functions of BMS is the lack of an effective way to obtain an exact state-of-charge (SOC). Moreover, the detection of the initial SOC (SOC_0) is rarely specifically mentioned. The SOC estimation system as a general multivariable function is a nonlinear, time-varying, strong coupling variable that virtually increases the difficulty of application.[2] Unfortunately, the SOC cannot be measured directly; it is estimated from other variables. Therefore, an assortment of methods is proposed in the literature or patent to measure or estimate the SOC. Generally speaking, such methods are divided into direct or indirect approaches. A widely used method for estimating the SOC is the ampere-hour (Ah) model, which is a required dynamic current with a time integral for SOC estimation.[3,4] This approach can be easily implemented in all portable devices as well as EV and HEV. However, it faces drawbacks such as accumulated current measurement error and inaccurate initial SOC(SOC_0)values. The indirect method for SOC estimation is based on the battery's SOC as a function of an inherent relationship such as open circuit voltage (OCV) and impedance. The OCV can provide useful information to the SOC based on intrinsic characteristics, and the OCV can naturally decline proportionately with the energy expenditure.[5−7] However, it is difficult to use a direct OCV model for the online application on account of the long waiting time that

Received: May 16, 2013
Revised: November 24, 2013
Published: December 18, 2013

is caused by the relaxation effect of the battery. The internal resistance of lithium-ion batteries is insensitive to SOC variation within the safe range of usage. Nevertheless, the Ah model or OCV mode has no such limitation.[8]

In this work, we estimate the SOC of $LiFePO_4$ rechargeable batteries and use the respective advantages of the OCV model and Ah model. The main contributions of this paper are the following: First, considering the advantages of the OCV to Ah model, an enhanced SOC_0 mode is designed. Second, the derivation of an enhanced SOC_0 model is a multiparameter function. Furthermore, the relaxation effect is paid more attention. Third, we propose an algorithm procedure to address how long it takes the concentration gradient (relaxation effect) of battery to disappear. Thus, the terminal voltage could be used as the open circuit voltage in OCV model, and the time constant could be expressed with a simple Thevein battery model and system identification. The outline of the paper is as follows: In Section 2, we briefly describe the SOC estimation model and experimental equipment and point out the key improvement parameters for the Ah model. In Section 3, we present a new SOC_0 model for $LiFePO_4$ batteries. Previous studies in this field ignore the effect of temperature, current rate, and relaxation effect generated in practical applications of the SOC_0 to the Ah model. In this paper, we address this shortcoming and additionally derive the function relationship between the time constant and time required for the terminal voltage to remain steady based on a model of the battery. In Section 4, the capacity efficiency based on the working model is applied to further improve the estimation accuracy of SOC online. In Section 5, dynamic stress test and comparison models based on the main improvement parameters will be presented to verify the superiority of the proposed algorithm.

AMPERE-HOUR (AH) MODEL AND TESTING BENCH

Ampere-Hour (Ah) Model. SOC estimation is significantly important for excavating the potentiality of the battery and is the emphasis and difficulty of BMS. Generally, SOC is defined as the ratio of releasable capacity, $Q_{releasable}$, relative to the rated capacity, Q_{rated}, during the profiles

$$\mathrm{SOC} = \frac{Q_{\mathrm{releasable}}}{Q_{\mathrm{rated}}} \times 100\% = \left(1 - \frac{Q_{\mathrm{consumption}}}{Q_{\mathrm{rated}}}\right) \times 100\% \quad (1)$$

Note that only releasable capacity can be calculated from eq 1 if discharged from a full capacity battery. Generally, the SOC is determined by the current integrating model (Ah model) and expressed as follows

$$\mathrm{SOC}(t) = \mathrm{SOC}_0 - \frac{1}{Q}\int_{t_0}^{t_1} \frac{1}{\eta} i\,dt \quad (2)$$

where SOC (t) is SOC as a function of time; SOC_0 is the initial state-of-charge; Q is the capacity, defined as the product of the current and time and as a function of temperature; η is the capacity efficiency; i is positive for discharging and negative for charging.

Test Bench. A $LiFePO_4$ battery module with nominal 3.20 V and nominal capacity of 20Ah is selected for the experiments. The test bench consists of a battery charging system (LAND-CT2001B, LAND Electronics Corp., China), battery discharging system (ITECH-IT8516, ITECH Limited), data acquisition system (Agilent 34970A, Agilent Limited), and a host computer with built in software for online programming charge and discharge. The host computer is used for the real-time calculation of the experiment parameters. The ITECH-IT8516 can discharge a battery according to the designed program and record various data such as current, voltage, and temperature. The experiment signals are monitored and recorded by data acquisition modules and then processed in a personal host computer. Furthermore, the data collection system Agilent 34970A is used, with a measurement accuracy of DC voltage as high as 0.15 mv.

SOC_0 MODEL

Traditional OCV Model. Following and tracking some useful methods of the traditional testing steps, discharge−resting−discharge, an effective method for the OCV test is proposed. In order to explore the changes of OCV at the different points of SOC, the following experiment was carried out. In the experiment, the battery is first charged with a constant current rate of 0.3 C to a threshold of 3.65 V, and then by a constant voltage of 3.65 V until the current rate decreases to 0.002 C. Subsequently, the battery voltage decreases gradually and reaches the designed capacity (SOC = 10−90%) with constant discharging rates. Moreover, the battery needs to rest for several minutes in order to facilitate the overall disappearance of the electrochemical polarization and concentration polarization.

In the practical application, the interrelationship between SOC and OCV was estimated, and the value of SOC could be used as the initial SOC for the Ah model. The traditional relationship between SOC and OCV is shown in Figure 1 and

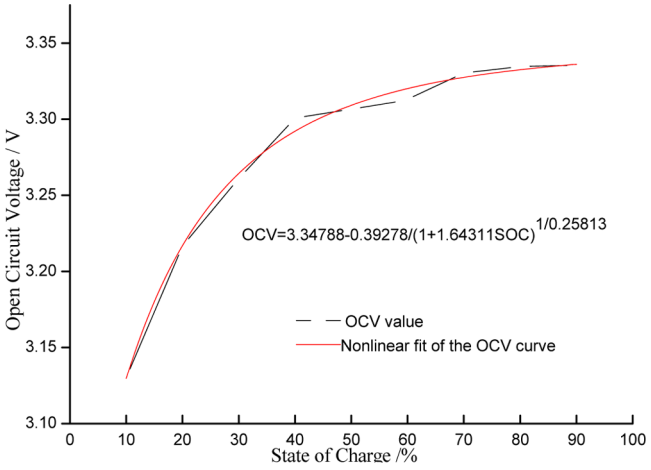

Figure 1. Discharging voltage with respect to SOC.

the function as eq 3. However, the long waiting time for the battery to reach a steady state must be considered; otherwise, it will cause the illusion of "virtual high" capacity in the SOC estimation. To improve the accuracy and speed of SOC_0, an enhanced OCV model for SOC_0 estimation is proposed and also takes into account the effect of resting time.

$$\mathrm{OCV} = 3.34788 - \frac{0.39278}{(1 + 1.64311\ \mathrm{SOC})^{1/0.25813}} \quad (R^2 = 99.7) \quad (3)$$

Effect of Relaxation Effect on SOC_0. In order to facilitate the overall disappearance of the polarization phenomenon and to solve the various theoretical and practical problems in SOC

dx.doi.org/10.1021/sc400430e | ACS Sustainable Chem. Eng. 2014, 2, 599−605

estimationthat we are facing today, the relaxation effect must be considered. The relaxation effect is due to the concentration gradient of active materials at the electrolyte−electrode interface and is formed by the electrochemical reactions during discharge. However, the length of the resting time is another arrestive and urgent problem. We experiment with the relationship between the resting time and the terminal voltage during discharging using a similar approach of pulse discharge. First, we use a conventional Thevenin model to simulate the dynamic behavior of the battery and the main model parameters. Then, the pulse discharge method is conducted, and mathematical functions of the terminal voltage are given for the stages of discharge and resting. Subsequently, the resistance and capacitance are obtained with system identification method in the above two stages. Lastly, the maximum number between the two time constants ($\tau = RC$) is used to determine the resting time for the terminal voltage.

Battery dynamic characteristics are described in the Thevenin model that consists of resistance R_0, R_k, R_d, and capacitance elements C_k and C_d. The Thevenin model fulfills its duties well in describing the electrical properties of batteries especially for the $LiFePO_4$ batteries; the schematic diagram of the models are shown in Figures 2[9,10] and 3, where V_t is the terminal voltage; I

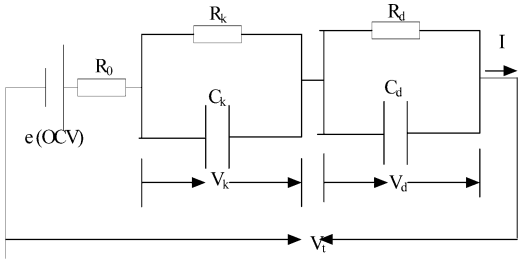

Figure 2. Schematic diagram for the Thevenin model.

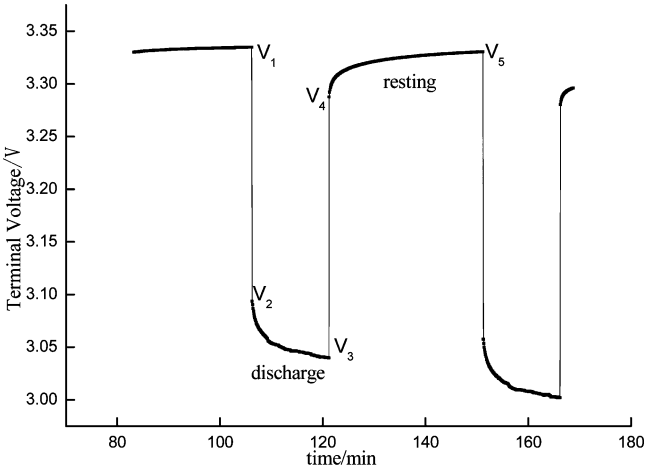

Figure 3. Schematic diagram of the model.

is the load current with a negative value during charge and a positive during discharge; R_k and R_d are the polarized resistances; C_k and C_d are the polarized capacitors in order to give a much more detailed description of polarization characteristic; V_k and V_d are the voltages across C_k and C_d, respectively; and ε is the open circuit voltage that refers to the equilibrium potential of the battery.

During the discharging stage, the electro-chemical polarization and concentration polarization states will appear once the batteries begin to discharge. This process is called the zero state response and is the behavior or response of a circuit with the initial state of zero with the electrical circuit theory. In other words, the capacitor has no initial energy storage before the current through its parallel resistance. With the prolonging of the discharging time, the voltage of V_k and V_d is rising gradually. So with an increase in discharge time, the voltage of the battery V_t is on a downward trend. Resistance is determined by the change of voltage and current using the following expression

$$R_0 = \frac{\Delta U}{\Delta I} = \frac{V_1 - V_2}{\Delta I} \tag{4}$$

The terminal voltage is expressed as

$$\begin{cases} V_t = \varepsilon - IR_0 - V_k - V_d \\ V_k = IR_k(1 - e^{-t/\tau_k}) \\ V_d = IR_d(1 - e^{-t/\tau_d}) \end{cases} \tag{5}$$

During the resting stage, with an increase in resting time, the terminal voltage is rising gradually. When there is no current through the resistance, the polarization phenomena will slowly disappear with time. This greatly increases the difficulty of the SOC_0 estimation when using the open circuit voltage (OCV) method. Under this stage, the terminal voltage is supplied by the charge stored in the capacitor during the resting time. The capacitor will be exponentially discharged with the corresponding circuit. It is a difficult problem when using the OCV model, which has yet to be adequately resolved. The terminal voltage can be expressed as

$$\begin{cases} V_t = \varepsilon - V_k - V_d \\ V_k = V_{k0}e^{-t/\tau_k} \\ V_d = V_{d0}e^{-t/\tau_d} \end{cases} \tag{6}$$

On the basis of the analysis of the voltage response with the pulse discharge experiment, parameter identification was carried out for the Thevenin model. The entire process of parameter identification is shown in Figure 4. The main parameters of resistance and capacitor can determined in terms of the experimental and/or simulation data based on eqs 4−6.

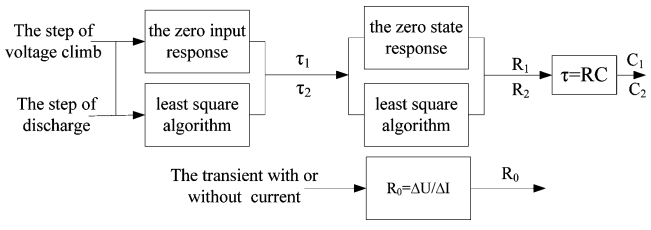

Figure 4. Flowchart of parameter identification in battery mode.

At the resting stage, the response of voltage (V_3−V_2) can be used to indicate voltage rebound change in the pulse discharge curve. With the actual voltage response values and the expressions of the voltage response ($V_{k0}e^{-t/\tau_k} + V_{d0}e^{-t/\tau_d}$), we can label the main parameters (τ_k,τ_d) as undetermined coefficients. Subsequently, the least-squares curve-fitting algorithm is used to solve these undetermined coefficienst.

At the discharging stage, the voltage response on the two RC circuits is $V_k + V_d = IR_k(1 - e^{-t/\tau_k}) + IR_d(1 - e^{-t/\tau_d})$. Putting formerly solved τ_1 and τ_2 into the above voltage expression and

dx.doi.org/10.1021/sc400430e | ACS Sustainable Chem. Eng. 2014, 2, 599−605

voltage drop in the two RC circuits, in combination with the least-squares curve-fitting algorithm, the values of $R1$and R2 are solved, as are C_k and C_d ($c = \tau/R$). Moreover, clearly a dissected identification method can also be seen in refs 11 and 12.

When the pulse current is removed, the terminal voltage is equal to the voltage on the capacitor (V_k+V_d). The stored charge on the capacitors C_k and C_d may be discharged through resistance R_k and R_d and then gradually disappears with extension of the resting time, respectively. In other words, the float voltage will gradually decrease to the equilibrium state. In addition, the external expression of the terminal voltage is increasing slowly and finally reaching the steady state. However, how long will it take for the terminal voltage to reach a steady state? Although a lot of effort is being spent on improving these weaknesses, an effective method has yet to be developed. It may require considering the time constant with the circuit theory.

The physical meaning of the time constant is the time of the voltage of the energy storage element up to 63.2% of the steady voltage between the initial and final values as shown in Figure 5.

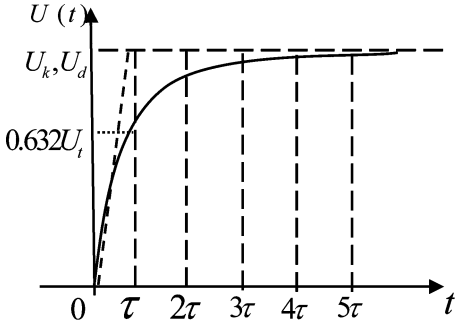

Figure 5. Capacitor voltage with time constant.

In addition, the time constant of an RC circuit is the product of the resistance and the capacitance; in other words, it could be obtained by the voltage curve.[13] The resting time is about 4−5 τ in this experiment.

The terminal voltage is gradually rising in the resting time and eventually reaches a steady value as the current is over. Taking 0.4 C (discharge rate) as the case in the research, it explores the interrelationship and the interplay between the SOC and open circuit voltage. The result is shown in Figure 9.

As shown in Figure 6, the voltage of the $LiFePO_4$ battery for resting for several seconds is far lower than that of resting for 30 min under the same current rates. As an overpotential of stopping discharge, the OCV naturally declines proportionately with the capacity lost and the SOC. Stopping the moment under the same SOC, the voltage of SOC90% (3.31 V) is significantly higher than other SOC (the voltage of SOC10% is only 3.18 V). Under the same SOC, the terminal voltage was gradually raised and eventually did not change significantly with the prolonged resting time. Thus, using only the OCV model to estimate the initial SOC is difficult because of voltage drift and the uncertainty of dispelling time. The OCV difference for the battery is only 1 mv with a resting time up to 25−30 min under 0.4 C discharge as illustrated in Figure 6. So, the relaxation effect is the most important influence factor to the SOC_0 estimation.[14]

Effects of Relaxation Effect and Discharge Rates on SOC_0. The subsequent step explores the interrelationship of the OCV and SOC under different discharge rates and resting times. The results are shown in Figure 7.

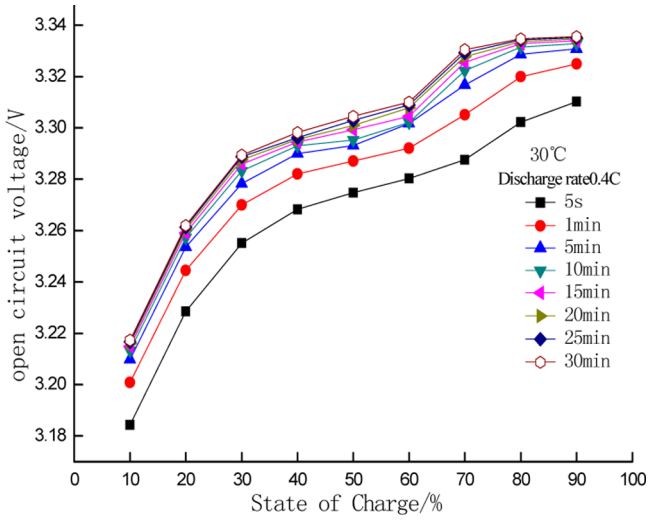

Figure 6. OCV versus SOC under different resting times (0.4 C).

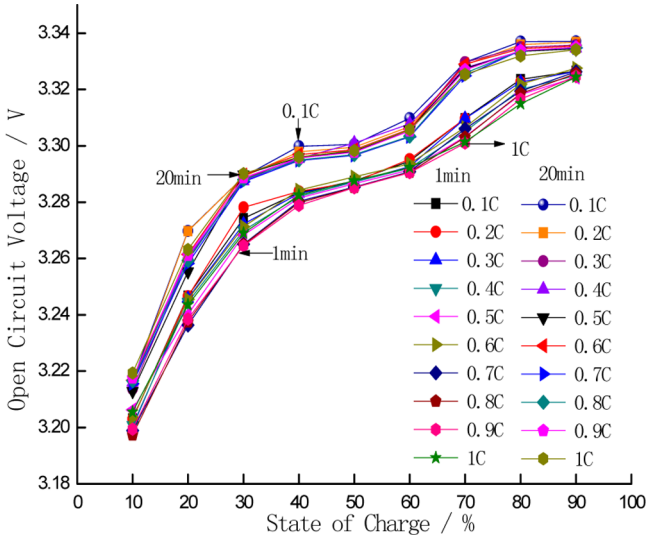

Figure 7. OCV vs SOC_0 under different resting times and discharge rates.

The voltage of the battery is climbing slowly and deliberately under different discharge rates, eventually close to an equilibrium state. A considerably higher correlation degree was established between the OCV and the resting time under the same SOC and discharge rate, respectively. The results showed that the higher discharge rate paid a greater effect on OCV than the lower one if under the same SOC and resting time. In the power-off moment, the discharge rate has a great effect on the OCV, especially in the scope of 20% to 80% SOC.

Effects of Multiparameters on SOC_0. The following discussions are on the SOC_0 estimation, which is based on the main impact parameters including real-time voltage, resting time, and discharge rates. Establishing an effective method for SOC_0 has profound significance to enhance estimation accuracy and realize its potential. Experimental data reflecting the interrelationship among the resting time, open circuit voltage, and SOC_0 are shown in Figure 8. Therefore, SOC_0 is estimated based on the value changes of the OCV and the resting time.

To further explore the influence of the discharge rate and OCV upon SOC_0, the improved SOC_0 model was demon-

dx.doi.org/10.1021/sc400430e | ACS Sustainable Chem. Eng. 2014, 2, 599−605

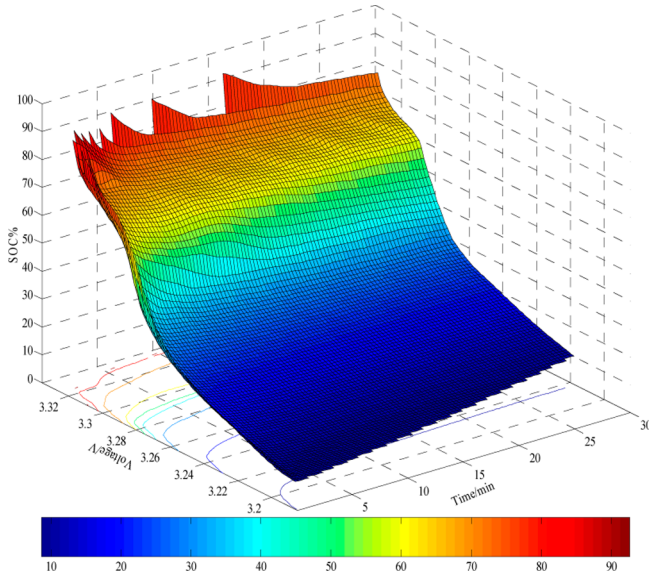

Figure 8. Resting time and terminal voltage with SOC (0.4 C).

strated with experimental data with various voltages and discharge rates. The interrelationships are shown in Figure 9.

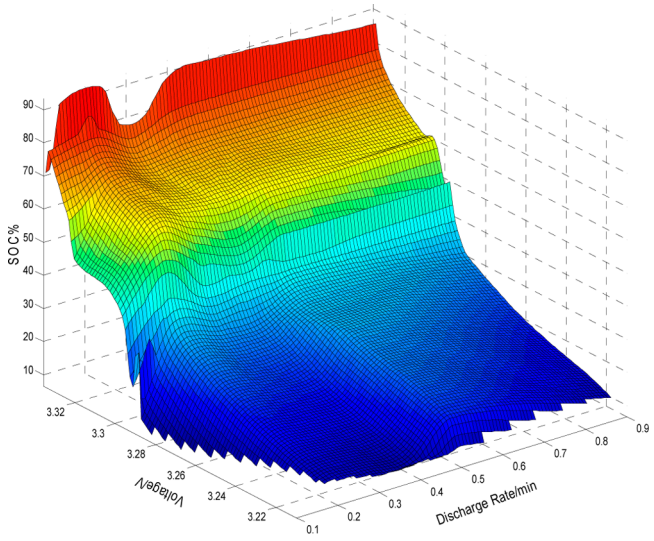

Figure 9. Discharge rate and terminal voltage with SOC (resting time = 20 min).

The dynamic performance of SOC_0 depends mainly on the parameters such as open circuit voltage (OCV), discharge rate (I), and the resting time (t). According to the invariance of the perfect differential form, it is expressed as eq 7

$$\mathrm{OCV} = f(\mathrm{SOC}_0, I, t) = k_1 \frac{\partial \mathrm{OCV}}{\partial \mathrm{SOC}_0} \frac{\partial \mathrm{SOC}_0}{\partial t} + k_2 \frac{\partial \mathrm{OCV}}{\partial I} \frac{\partial I}{\partial t} \tag{7}$$

The weighted coefficient (k_1,k_2) is a dynamic change parameter in the SOC estimation. However, the differential function further increased computational complexity and the hardware requirements of BMS. Parameter k_1 and k_2 can be determined with principal component analysis (PCA) and gray correlation, etc. They are a dynamic parameter and a function of various SOC.

According to the curve fitting of the multifaceted theory, the enhanced SOC_0 model can be expressed with polynomial regression that is used in this research and as a function of resting time, ambient temperature, open circuit voltage, and discharge rates.

CAPACITY EFFICIENCY

On the basis of electrochemical reaction kinetics, the discrepancy in capacity and energy of the batteries can be found and causes the discharging efficiency change in various discharge rates and SOC. Consequently, the capacity efficiencies of the battery need to be tested. Discharging experiments are conducted to obtain the discharging capacity efficiency, which is calculated by

$$\eta_2 = \frac{Q_{\mathrm{discharge,0.1C-1C}}}{Q_{\mathrm{charge,0.3C}}} \times 100\% \tag{8}$$

The results indicate that the relationship between the discharging capacity and the rated capacity is a linear relation in some scope of rate, as shown in Figure 10. As a result, the capacity efficiency can be expressed in terms of discharge rate.

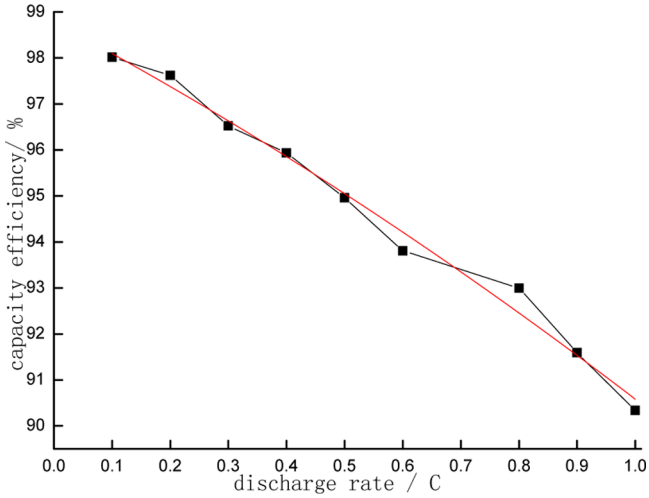

Figure 10. Capacity efficiency with discharge rate.

On the basis of the minimum mean square error, the curve fitted quadratic expression of capacity efficiency as a function of current could be expressed as

$$\eta_2 = 0.9875 - 3.374 \times 10^{-3} i - 3.709 \times 10^{-5} i^2 \tag{9}$$

The experimental results of capacity efficiency show a significant negative correlation between the capacity efficiency and the discharge rate. Furthermore, the capacity efficiency is greater than 90%. From above, it can be seen that the capacity efficiency is not suitable for simplification to 100%; otherwise, big errors may be introduced.

The relationship between capacity efficiency and SOC is investigated in the state of different SOC and the same discharge rate. The result was shown in Figure 11. The test results show that the influence of SOC on capacity efficiency is weak and hardly changes. Therefore, the effect of capacity efficiency to SOC can be negligible.

dx.doi.org/10.1021/sc400430e | ACS Sustainable Chem. Eng. 2014, 2, 599−605

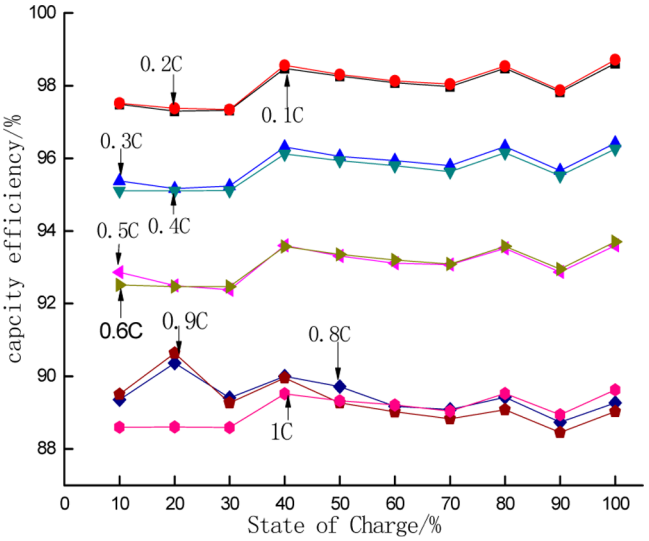

Figure 11. Capacity efficiency with SOC.

MODEL VALIDATION TEST

For evaluating the reliability of the enhanced SOC_0 model, the verification test is required. To verify the proposed SOC_0 model and parameters of the model, DST profiles and analysis were performed. On the basis of an accurate and simple estimation of the enhanced OCV model, a robust OCV−Ah model is built with an intrinsic relationship of the battery. Herein, the DST cycle is selected for the experiment to verify the capability of the proposed model at ambient temperature. The DST cycle and its related battery current and voltage are shown in Figure 12.

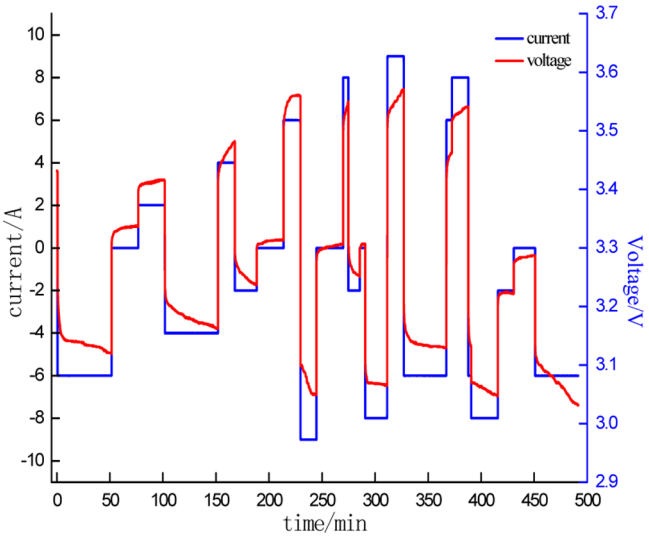

Figure 12. Plots of DST test: voltage−time profiles and current−time profiles.

The comparison of the relative models is shown in Figure 13. It is performed between the various online estimation models including OCV−Ah, OCV−Ah−η, and enhanced OCV−Ah−η. The performance results through the discharge test after the cycles come within the specifications is shown in Figure 14.

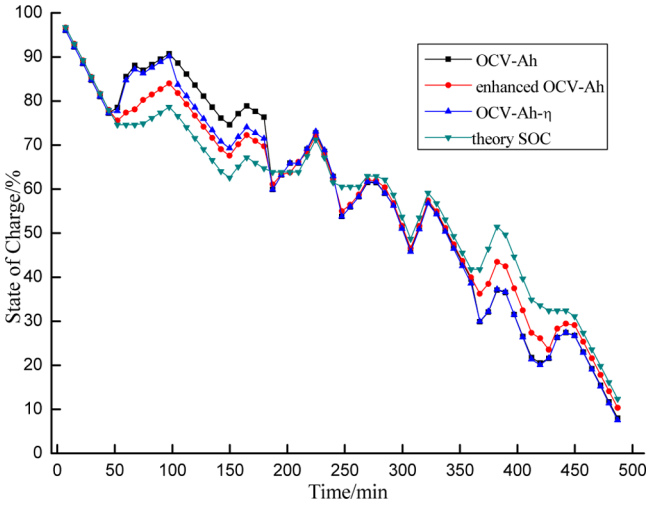

Figure 13. SOC estimation error curves of the three methods.

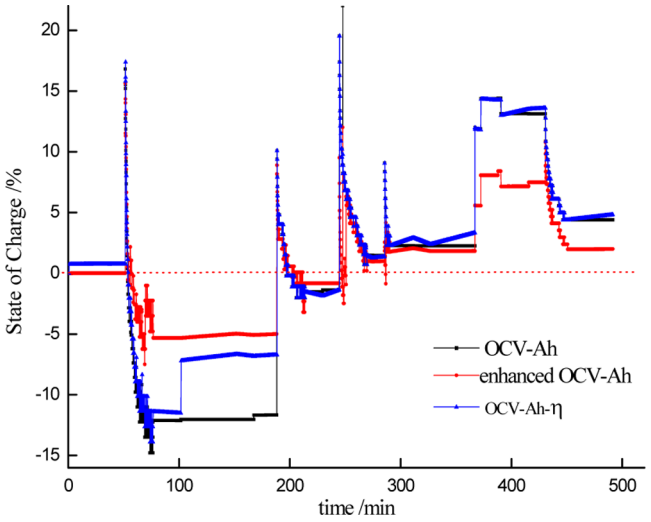

Figure 14. Error comparison of the three methods under the DST test.

CONCLUSIONS

An enhanced SOC_0 estimation model that based on the traditional OCV method was implemented and verified experimentally for the $LiFePO_4$ battery. To improve the SOC estimation accuracy of the Ah model, the correction of the discharge efficiency of the battery was considered. On the basis of the above analysis, the main noteworthy conclusions are as follows:

(1) An equivalent circuit model is proposed to describe the dynamic characteristics of the $LiFePO_4$ battery, and its mathematical equations are justifiable based on the indispensable simulation of the polarization characteristic. Comparative analysis on the terminal voltages are conducted between the simulation and the online estimation under the intermittent discharge test.

(2) To improve the accuracy of estimation, an enhanced SOC_0 model is put forward and employed in the online SOC_0 estimation of the Ah model. It also puts forth that the practicability of the model should be mainly considered in the design of the approach. Also, the effects of voltage, current, and resting time for SOC_0 were mainly analyzed, and a model was established.

dx.doi.org/10.1021/sc400430e | ACS Sustainable Chem. Eng. 2014, 2, 599−605

(3) The influence of temperature was considered for the proposed estimation method of SOC_0 and capacity. The influence of temperature on the OCV (open circuit voltage) model is far less than the capacity. The enhanced SOC_0 model is implemented merely based on the terminal voltage, last load current, and the resting time without the influence of such disturbances as the ambient temperature and working history of the battery. The accuracy and robustness can be guaranteed easily.

(4) The estimation characteristics of the various enhanced OCV−SOC model is compared using the measurement data acquired from a commercial $LiFePO_4$ battery on the test bench. DST test cases designed to soundness verify the enhanced model, and the results indicate that it is simply in computational complexities and easier to realize with hardware for BESS applications without the requirements of a large-memory and high quality CPU. The experimental results of the online SOC estimation based on robust the OCV−SOC model can efficiently restrict the error for DST cycles.

The multiparameter initial state-of-charge model that is reasonable and has good performance is presented for application in EV/HEV/PHEV. It is easily implemented with a simple calculation for the battery management system.

AUTHOR INFORMATION

Corresponding Author

*E-mail: songwj@ms.giec.ac.cn; zhangyh@ms.giec.ac.cn, Tel.: +86-20-8705-9478, Fax: +86-20-8705-7795.

Notes

The authors declare no competing financial interest.

ACKNOWLEDGMENTS

This work is financially supported by National Natural Science Foundation of China (No.51206175)

REFERENCES

(1) Adams, S. Ultrafast lithium migration in surface modified $LiFePO_4$ by heterogeneous doping. *Appl. Energy* **2011**, *95*, 323−328.

(2) Reed, T. D.; Malcolm, D. M. Modeling the prospects of plug-in hybrid electric vehicles to reduce CO_2 emissions. *Appl. Energy* **2011**, *88*, 2315−2523.

(3) Aylor, J. H.; Thieme, A.; Johnso., B. W. A battery state-of-charge indicator for electric wheelchairs. *IEEE Trans. Ind. Electron.* **1992**, *39*, 398−409.

(4) Liu, T. H.; Chen, D. F.; Fang, C. C. Design and implementation of a battery charger with a state-of-charge estimator. *Int. J. Electron* **2000**, *87*, 211−226.

(5) Lee, S.; Kim, J.; Lee, J.; Cho, B. State-of-charge and capacity estimation of lithium ion battery using a new open-circuit voltage versus state-of-charge. *J. Power Sources* **2008**, *185*, 1367−1373.

(6) Ng, K. S.; Moo, C. S.; Chen, Y. P.; et al. Enhanced coulomb counting method for estimating state-of-charge and state-of-health of lithium-ion batteries. *Appl. Energy* **2009**, *86*, 1506−1511.

(7) He, H.-w.; Zhang, X. W.; Xiong, R.; et al. Online model-based estimation of state-of-charge and open-circuit voltage of lithium-ion batteries in electric vehicles. *Energy* **2012**, *39*, 310−18.

(8) Chiang, Y. H.; Sean, W. Y.; Ke, J. C. Online estimation of internal resistance and open-circuit voltage of lithium-ion batteries in electric vehicles. *J. Power Sources* **2011**, *196*, 3921−3932.

(9) Benini, L.; Castelli, G.; Macci, A.; et al. Discrete-time battery models for system-level low-power design. *IEEE Trans. VLSI Syst.* **2001**, *9*, 630−640.

(10) Gao, L.; Liu, S.; Dougal, R. A. Dynamic Lithium-Ion Battery Model for System Simulation. *IEEE Transactions on Components and Packaging Technologies* **2002**, *25*, 495−505.

(11) Wang, S.-q.; Verbrugge, M.; Wang, J. S.; et al. Multi-parameter battery state estimator based on the adaptive and direct solution of the governing differential equations. *J. Power Sources* **2011**, *196*, 8735−8741.

(12) Huria, T.; Ceraolo, M.; Gazzarri, J., et al. *High Fidelity Electrical Model with Thermal Dependence for Characterization and Simulation of High Power Lithium Battery Cells*. IEEE International Electric Vehicle Conference (IEVC), Greenville, SC, March 4−8, 2012.

(13) Vasebi, A.; Partovibakhsh; Bathaee, S. M. T. A novel combined battery model for state-of-charge estimation in lead-acid batteries based on extended Kalman filter for hybrid electric vehicle applications. *J. Power Sources* **2007**, *174*, 30−40.

(14) Zhang, Y. H.; Song, W. J.; Lin, S. L.; Feng., Z. P. A novel model of the initial state of charge estimation for $LiFePO_4$batteries. *J. Power Sources* **2014**, *248*, 1028−1033.